Supplementary Information for

Structural basis for the inability of chloramphenicol to inhibit peptide bond formation in the presence of A-site glycine.

Egor A. Syroegin[1,*], Elena V. Aleksandrova[1,*], and Yury S. Polikanov[1,2,3,#]

[1] Department of Biological Sciences, University of Illinois at Chicago, Chicago, IL 60607, USA

[2] Department of Pharmaceutical Sciences, University of Illinois at Chicago, Chicago, IL 60607, USA

[3] Center for Biomolecular Sciences, University of Illinois at Chicago, Chicago, IL 60607, USA

* Authors contributed equally to this work
[#] To whom correspondence should be addressed:

E-mail: yuryp@uic.edu (Y.S.P.)

This file includes:

I. Supplementary Table 1;

II. Supplementary Figures 1 to 3 with legends;

III. Supplementary References.

II. SUPPLEMENTARY TABLES

Table S1. X-ray data collection and refinement statistics.

Crystals	**70S ribosome complex with A-site Gly-tRNA^{Gly}, and P-site fMet-tRNA$_i^{Met}$ PDB entry 7U2H**	**70S ribosome complex with A-site Gly-tRNA^{Gly}, P-site fMet-tRNA$_i^{Met}$, and CHL PDB entry 7U2I**	**70S ribosome complex with A-site Gly-tRNA^{Gly}, P-site fMAC-tRNA$_i^{Met}$, and CHL PDB entry 7U2J**
Diffraction data			
Space Group	$P2_12_12_1$	$P2_12_12_1$	$P2_12_12_1$
Unit Cell Dimensions, Å (a x b x c)	210.61 x 451.44 x 624.84	210.17 x 450.98 x 624.13	209.93 x 451.24 x 622.35
Wavelength, Å	0.9792	0.9792	0.9791
Resolution range (outer shell), Å	226-2.55 (2.62-2.55)	255.49-2.55 (2.62-2.55)	174-2.55 (2.62-2.55)
I/σI (outer shell)	6.93 (0.93)	6.19 (0.93)	7.90 (0.89)
Resolution at which I/σI=1, Å	2.55	2.55	2.55
Resolution at which I/σI=2, Å	2.80	2.80	2.80
CC(1/2) at which I/σI=1, %	18.5	18.9	17.1
CC(1/2) at which I/σI=2, %	50.0	50.0	50.0
Completeness (outer shell), %	99.5 (99.8)	99.4 (99.8)	99.5 (100.0)
R_{merge} (outer shell)%	26.8 (236.4)	17.2 (150.6)	16.7 (228.1)
No. of crystals used	2	1	1
No. of Reflections Used:	19,099,952 1,896,410	7,719,767 1,887,449	11,553,376 1,882,520
Redundancy (outer shell)	10.1 (10.1)	4.09 (3.96)	6.14 (6.29)
Refinement			
Resolution range of the diffraction data included in the refinement, Å	146-2.55	154-2.55	125-2.55
R_{work}/R_{free}, %	21.4/26.2	21.7/26.7	20.7/25.5
No. of Non-Hydrogen Atoms			
RNA	200,527	200,527	200,507
Protein	90,976	90,976	90,998
Ions (Mg, K, Zn, Fe)	2,850	2,850	2,851
Waters	5,045	5,045	5,042
Ramachandran Plot			
Favored regions, %	91.32	91.25	91.20
Allowed regions, %	8.47	8.48	8.58
Outliers, %	0.21	0.26	0.22
Deviations from ideal values (RMSD)			
Bond, Å	0.008	0.008	0.009
Angle, degrees	1.408	1.410	1.454
Chirality	0.058	0.058	0.059
Planarity	0.007	0.007	0.008
Dihedral, degrees	17.305	17.457	17.408
Average B-factor (overall), Å^2	57.7	61.7	70.9

II. SUPPLEMENTARY FIGURES

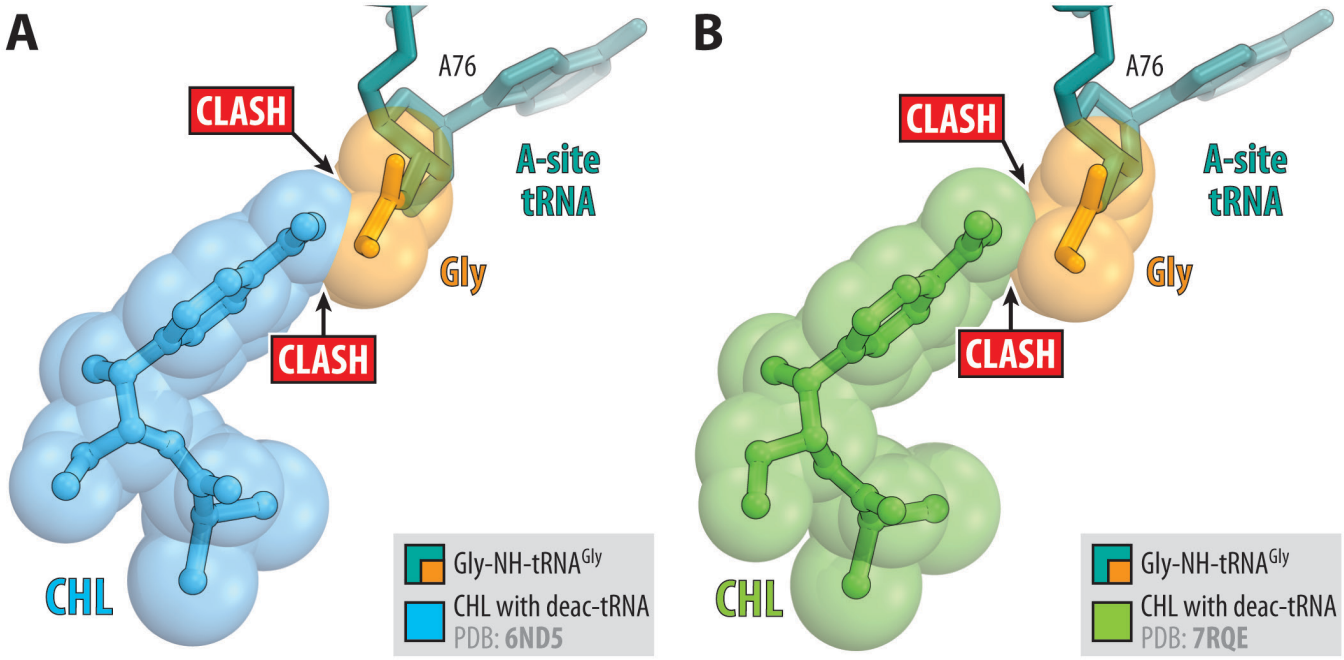

Figure S1. Alignments of the glycyl-tRNA structure with those of the ribosome-bound CHL. (A, B) Superpositioning of the 70S ribosome structure carrying Gly-NH-tRNA^{Gly} (teal with glycyl moiety highlighted in orange) and fMet-NH-tRNA$_i^{Met}$ (omitted for clarity) in the A and P sites, respectively, with the previously reported structures of ribosome-bound CHL in the presence of full-length deacylated tRNAs in both A and P sites (A, PDB entry 6ND5 (1)) or short deacylated A-site tRNA and P-site peptidyl-tRNA analogs (B, PDB entry 7RQE (2)). All structures were aligned based on domain V of the 23S rRNA. Note a clash between the main-chain Cα atom of the glycine residue and the nitrobenzyl moiety of CHL.

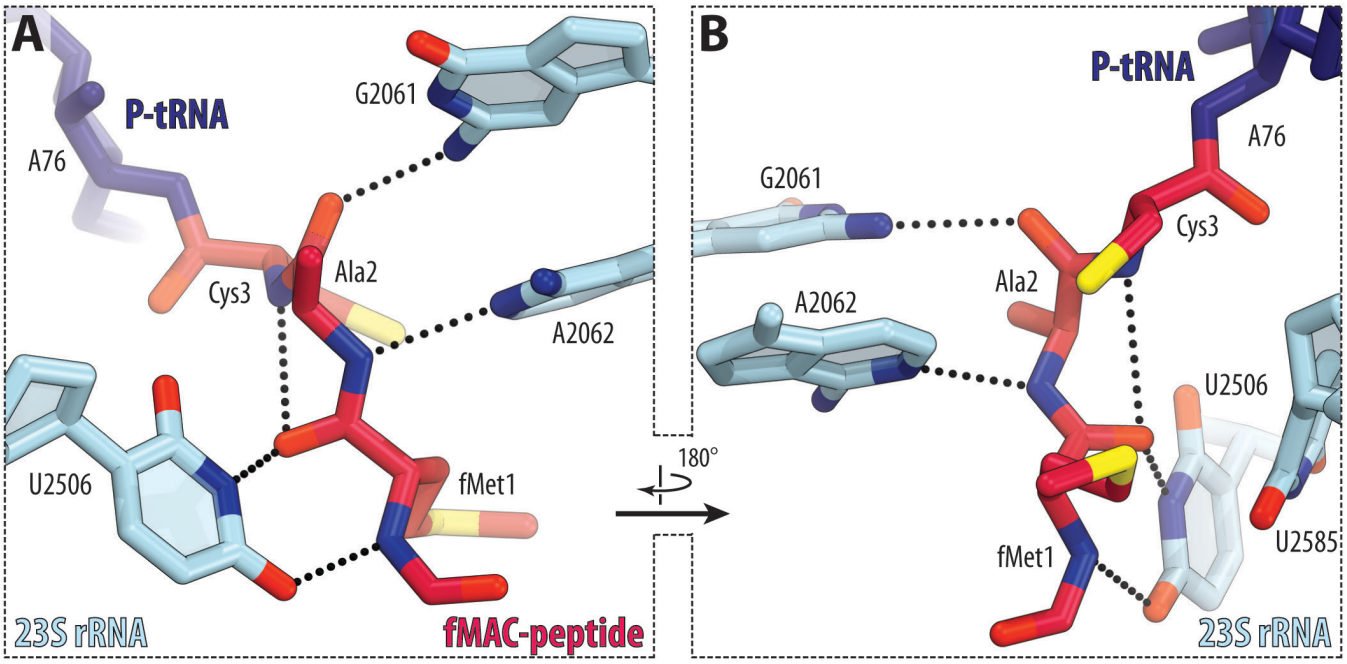

Figure S2. Tight coordination of the fMAC-peptidyl-tRNA in the nascent peptide exit tunnel. (A, B) Close-up views of the interactions between the ribosome-bound fMAC-peptidyl-tRNA (navy with peptidyl moiety highlighted in crimson) and the nucleotides of the 23S rRNA (light blue). H-bonds are shown by black dotted lines. Nitrogen atoms are shown in blue, oxygens are red, and sulfurs are yellow.

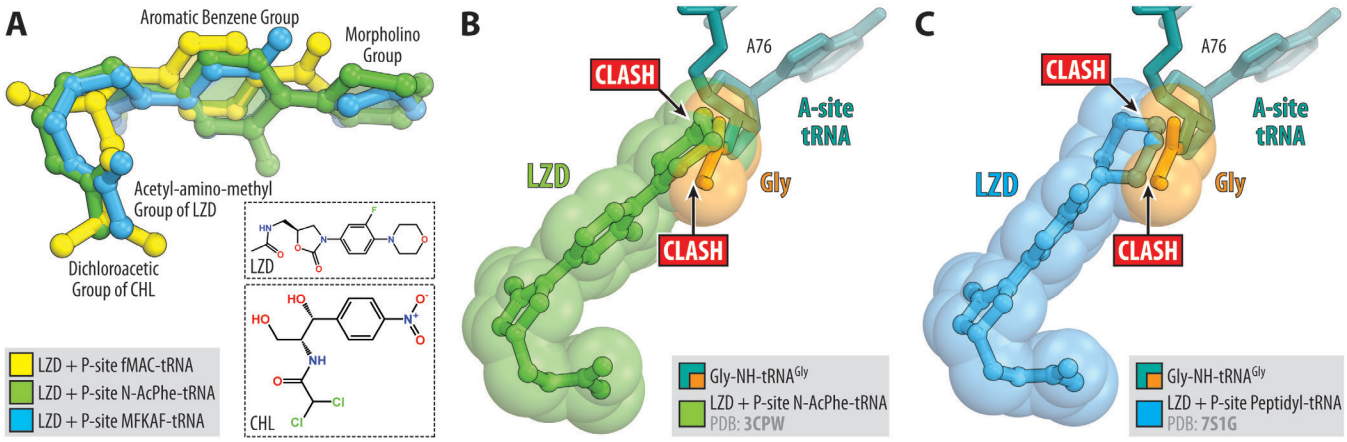

Figure S3. Alignment of the glycyl-tRNA structure with those of the ribosome-bound LZD. (**A**) Superposition of the new structure of CHL (yellow) with the previous structures of ribosome-bound LZD in the presence of P-site N-AcPhe-tRNA analog (green, PDB entry 3CPW (3)) or full-length P-site MFKAF-peptidyl-tRNA (blue, PDB entry 7S1G (4)). All structures were aligned based on domain V of the 23S rRNA. Note that the aromatic rings of these two chemically unrelated drug molecules superimpose well with each other. (**B, C**) Superpositions of the 70S ribosome structure carrying Gly-NH-tRNA^{Gly} (teal with glycyl moiety highlighted in orange) and fMet-NH-tRNA$_i^{Met}$ (omitted for clarity) in the A and P sites, respectively, with the previous structures of ribosome-bound LZD shown in panel A. Note a prominent clash between the main-chain atoms of the glycine residue (as well as the ribose of A76 nucleotide) and the morpholino moiety of LZD.

III. SUPPLEMENTARY REFERENCES

1. Svetlov, M.S., Plessa, E., Chen, C.W., Bougas, A., Krokidis, M.G., Dinos, G.P. and Polikanov, Y.S. (2019) High-resolution crystal structures of ribosome-bound chloramphenicol and erythromycin provide the ultimate basis for their competition. *RNA*, **25**, 600-606.

2. Syroegin, E.A., Flemmich, L., Klepacki, D., Vazquez-Laslop, N., Micura, R. and Polikanov, Y.S. (2022) Structural basis for the context-specific action of the classic peptidyl transferase inhibitor chloramphenicol. *Nat. Struct. Mol. Biol.*, **29**, 152-161.

3. Ippolito, J.A., Kanyo, Z.F., Wang, D., Franceschi, F.J., Moore, P.B., Steitz, T.A. and Duffy, E.M. (2008) Crystal structure of the oxazolidinone antibiotic linezolid bound to the 50S ribosomal subunit. *J. Med. Chem.*, **51**, 3353-3356.

4. Tsai, K., Stojković, V., Lee, D.J., Young, I.D., Szal, T., Vazquez-Laslop, N., Mankin, A.S., Fraser, J.S. and Fujimori, D.G. (2022) Structural basis for context-specific inhibition of translation by oxazolidinone antibiotics. *Nat. Struct. Mol. Biol.*